

## EFFECT ON MECHANICAL DAMAGE ON CASTOR GERMINATION AND DAMAGE DETECTION METHOD

### 机械损伤对蓖麻种子发芽影响试验及损伤检测研究

Junming HOU, Enchao YAO, Hongjie ZHU, Weixue HU, Zhaotan REN

Shenyang Agricultural University, College of Engineering / China;

Tel: +86024-88487116; E-mail: junming\_hou@163.com

DOI: <https://doi.org/10.35633/inmateh-68-24>

**Keywords:** Castor seed; Mechanical damage; Germination; Image processing

#### ABSTRACT

To study the types of mechanical damage for castor seeds and their effects on germination, the image processing method was applied to detect the damage affecting germination. Two typical varieties of castor were selected for test. The type of mechanical damage of castor seeds was taken as the factor, the germination rate and germination vigor index were selected as indicators for one-way analysis of variance. The effects of mechanical damage on the germination of castor seeds were analyzed. Different algorithms were applied to extract the features of cracks and seed shell missing, and the corresponding defect parameters were calculated. The results showed that the effects of mechanical damage on the germination rate, germination potential, germination index, and vigor index of castor seeds were significant. The endosperm damage seriously affected the activity of castor seeds and seriously hindered seed germination. According to the analysis of the shell, some castor seeds cracked or there was incomplete shell damage at the same time, the internal endosperm being also damaged. The actual crack length was compared with the length measured by the ultra-depth of field microscope, which found that the margin of error was about 25% and the better error was 10%. Through the morphological processing, it could completely extract the characteristics of castor seed image without seed shells. The error between the extracted feature area and the measured object area function of the super depth of field microscope is about 10%.

#### 摘要

为了研究蓖麻种子机械损伤类型及其对发芽的影响，并通过图像处理手段对损伤进行检测。选用两种典型材料试验，以蓖麻种子机械损伤类型为因素，以发芽率、发芽势、活力指数等为指标做单因素方差分析，分析机械损伤对蓖麻种子发芽的影响。最后通过不同算法对裂纹与种壳缺失进行特征提取，并计算相应的缺陷参数。研究表明，机械损伤对蓖麻种子的发芽率、发芽势、发芽指数及活力指数影响显著；胚乳损伤严重影响蓖麻种子的活性，严重阻碍种子发芽；根据去壳分析，部分蓖麻种子产生裂纹或者种壳不完全损伤的同时，内部胚乳也产生了损伤，从而导致它们与完整蓖麻种子之间发芽率差异显著。将检测实际裂纹长度与超景深显微镜测量长度比较，可以看出误差范围基为 25%，比较优异的误差为 10%。通过最大类间方差法对种壳缺失的蓖麻种子进行图像分割，并通过形态学处理后，能将种壳缺失蓖麻种子图像的特征完全提取出来，提取到的特征面积与超景深显微镜的实测物体面积功能的误差为 10%。

#### INTRODUCTION

Castor is an important biomass resource oil crop with high oil content, which can produce nylon, lubricants, surfactants, and other products, and has a wide range of applications in high-technology fields such as aviation, navigation, transportation, and pharmaceutical manufacturing (Li *et al*, 2018; Sun *et al*, 2012). The damage among castors is serious in the process of shelling. The slight deformation or external damage to the seed directly affect its germination rate and the growth of the plant (Yu *et al*, 2019).

The related aspects have been studied by scholars on other materials. Mechanical threshing causes various forms of internal damage to soybean (Gao *et al*, 2010). These damages seriously affect the germination rate of soybean seeds and their germination quality. Related studies have analyzed the relationship between the degree of mechanical damage and germination of maize seeds by different techniques (Zhang *et al*, 2014; Junior *et al*, 2019). It was found that the damage rate of maize seeds increased and seed viability decreased with the increase in seed water content during mechanical threshing

(Gu *et al*, 2019). It was deduced that split glumes and cracks led to lower germination potential and germination rate of rice seeds and lower seedling quality. The correlation analysis between plant height and the degree of pressure application was performed (Song *et al*, 2019). Related studies found that mechanical scratching and mechanical shelling process without injuring the inner part of the seeds can promote seed germination and water absorption. When the inner part was injured mechanical damage to some extent will inhibit seedling growth after germination, which also reduce seed dry weight to some extent (Ju *et al*, 2018; Ju *et al*, 2020). It is clear that when mechanical damage injures the inner part of the seeds, it inhibits seed germination. When the seeds are not injured inside, it can promote seed germination appropriately. When mechanical damage inhibits seed germination, seeds that cannot germinate need to be detected by image processing algorithms. Related studies acquired the defect images by the multispectral computer vision system, which combined with the corresponding traditional algorithm for defect detection. The method can obtain the defect information better and has a high defect detection rate (Che *et al*, 2020; Cheng *et al*, 2018; Luo *et al*, 2019). Some studies applied threshold segmentation methods for image segmentation of larger defects, which are good for obtaining larger defect information (Liu *et al*, 2017; Diao *et al*, 2018; Su *et al*, 2019; Henila *et al*, 2020). Edge detection algorithms can be used to obtain edge information and pinpoint edge locations, which also have better edge processing capabilities (Yang *et al*, 2021; Sangeetha *et al*, 2016; Wang *et al*, 2017; Ju *et al*, 2020; Han *et al*, 2020).

The study first carried out germination test on damaged castor seeds, and detected part of mechanical damage. In this study, castor widely planted in Tongliao region was selected as the research object. The damage types of castor seeds caused by actual shelling were analyzed. The effects of damage types on the germination rate, germination potential, germination index and vigor index of castor seeds were also studied. Finally, image processing algorithm was used to detect the defects of damaged castor seeds.

## MATERIALS AND METHODS

### Experimental material

Castor capsule was divided into two categories, which are thornless and thorny castors. TongBi No.9 was thorny and ZheBi No.4 was thornless. The material was collected from Tongliao city. Fig. 1 showed the schematic diagram of castor capsule and castor seeds.

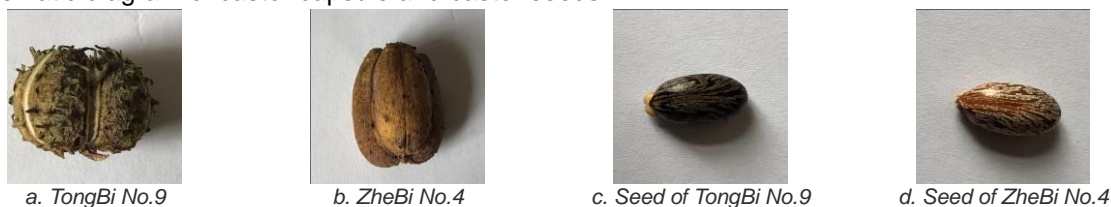


Fig. 1- Castor capsule and castor bean seed

### Castor seeds of different damage types

Castor seeds would produce some form of damage in the process of shelling. The damage was based on the actual condition of the material after shelling (Na *et al*, 2010). The castor seed damage characteristics was divided into five cases (Fig. 2).



Fig. 2 - Damage characteristics of castor oil seeds

They were shown as following: incomplete damage to the seed shell—castor seeds were missing part of the shell, the missing part to reveal the white endosperm (Fig. 2a). Complete damage to the seed shell—castor seeds were completely missing the shell—the white endosperm was completely exposed (Fig. 2b). Endosperm damage, when the seed shell was missing, the white endosperm was partially cracked or partially broken (Fig. 2c). Scaling—the epidermis of castor seed shell was peeling off (Fig. 2d). The cracking—the surface of castor seed shell was split (Fig. 2e).

### Test procedure

Selected mechanically damaged and complete castor seeds (seeds full and similar in size) of 30 each, soak in warm water at 40~50°C for 5~6 hours to soften the hard shell, so that the seeds absorb enough water to speed up seed germination. They were evenly put on a press cloth on a 60-millimeter petri dish. Each petri dish was filled with 5 milliliters of water, thus forming germination condition. The experiment was repeated three times. In the process of germination and growth, pour the same amount of water over the castor seeds every day. After 24 hours of germination promotion, the germination situation was observed (Seed germination occurs when the bud grows to about 3 millimeters). Then the germination of castor seeds was observed every 24 hours and the number of germinated seeds was recorded for a total of 7 to 9 days. The germination rate, germination potential, germination index, and vigor index were selected to test the quality of mechanically damaged castor seeds, then the effect of mechanical damage on germination was tested (Li et al, 2018; Joanna et al, 2018; Chiara et al, 2018).

$$\text{Germination rate (GP, \%)} = \frac{N_{8D}}{N_{TD}} \quad (1)$$

$$\text{Germination potential (GE, \%)} = \frac{N_{4D}}{N_{TQ}} \quad (2)$$

$$\text{Germination index (Gi)} = \sum_{i=1,2,\dots} \frac{N_{Di}}{D_i} \quad (3)$$

$$\text{Vital index (Vi)} = G_i * L \quad (4)$$

Where  $N_{8D}$  is the number of seeds germinated after 8 days.  $N_{TQ}$  is the total number of seeds per tray.  $N_{4D}$  is the number of seeds germinated after 4 days.  $N_{Di}$  is the number of seeds germinated on a day  $i$ .  $D_i$  is the number of days on the day  $i$ .  $L$  is the length of germinated seedlings.

### Statistical analysis for test

The results for each treatment group were three independent replicate trials, then the values for each experiment were expressed as mean  $\pm$  standard deviation (SD). One-way ANOVA method was used to determine the mean of the experimental data and the significance for each index, and the significance of differences between levels was determined according to the Duncan multiple comparison method with a significance level of 0.05.

### The results of the germination of castor seed

Take the castor seeds with the missing seed shell of TongBi No.9 as an example, and observe its germination and growth process for 6 days. After 6 days of germination, the number of germinated castor seeds had remained the same, so the growth could be observed for 6 days. Fig. 3 shows the germination and growth of castor seeds with missing seed shells.

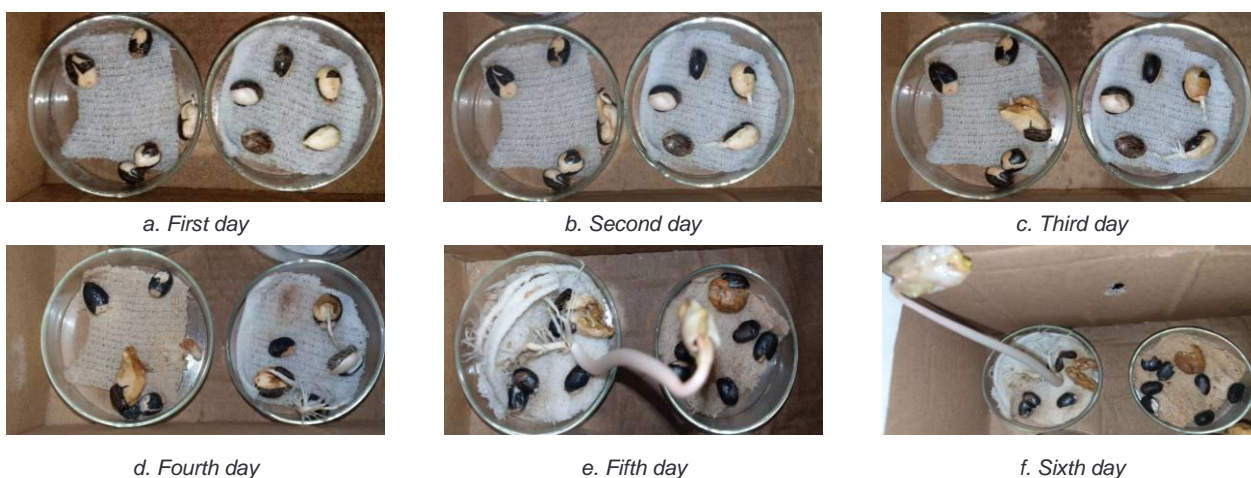


Fig. 3 - Germination and growth of castor seeds with missing shells

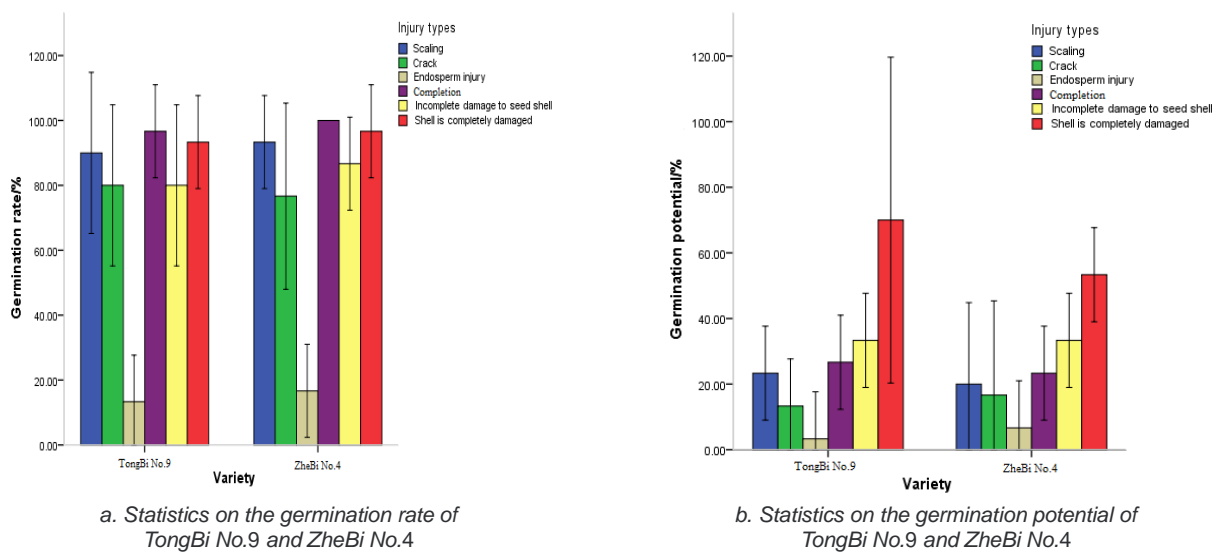
Fig. 3(a) shows the germination of castor seeds after one day. One castor seed had germinated and the radicle had grown on 5 mm, exposing the germ.

Fig. 3(b) shows the germination of castor seeds after two days. The germinated seeds already had four grains, but the pre-growth was slow and the radicle length is 8-10 mm. Fig. 3(c) shows the germination of castor seeds after three days, with one seed having grown many radicles. Fig. 3(d) is the growth of four days castor seeds with increasingly developed and dense root systems. Fig. 3(e) and Fig. 3(f) shows the growth of castor seed after five or six days, it had a thick main stem, cotyledons gradually unfolded, cotyledons and root system grew well.

**RESULTS AND DISCUSSION**

**Effect of mechanical damage on germination rate and germination potential**

The germination rate and germination potential of seeds were important indicators of seed quality. Fig. 4 shows the statistical graphs of germination rate and germination potential of TongBi No.9 and ZheBi No.4. It could be observed that the germination rate and germination potential of the two varieties seeds had the same distribution. The germination rate and germination potential of each damage type were not different. They were the highest germination rate of complete castor seeds and the lowest germination rate of endosperm damaged castor seeds. It shows that the variety has little effect on germination rate and germination potential.



**Fig. 4 - Statistics of the germination rate and germination potential of TongBi No.9 and ZheBi No.4**

It could be found that the effect of variety on germination rate and germination potential was not significant. Then the dynamic analysis and table analysis were conducted with TongBi No. 9 as an example. Fig. 5 shows the relationship between germination rate and germination potential of castor seeds under different damage types of TongBi No.9.

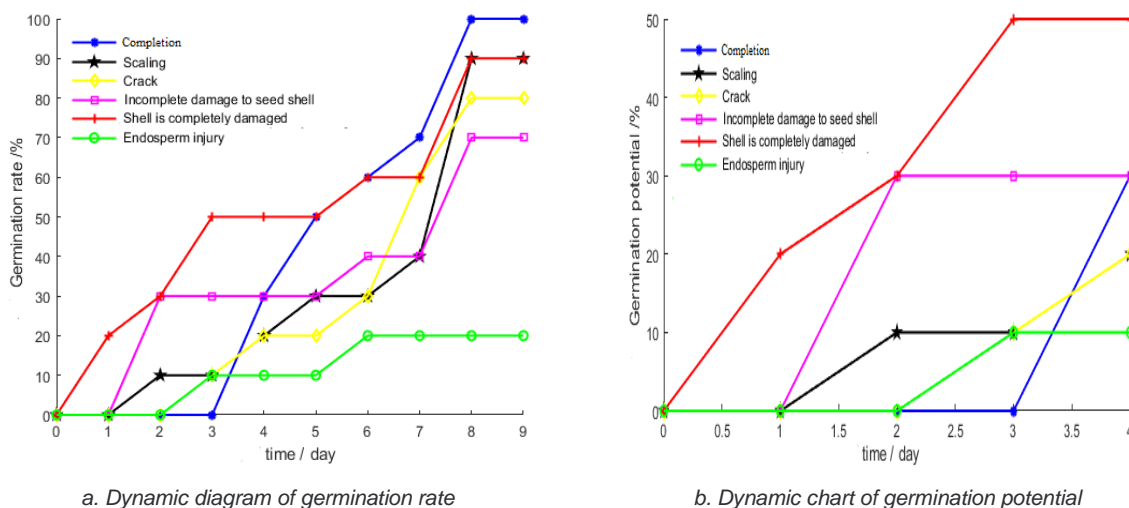


**Fig. 5 - Germination rate and germination potential of castor oil seeds**

It could be found that castor seeds with partial and complete damage to the seed shell germinated earlier than other castor seeds. They had higher germination potential than other damage types of castor seeds. The growth dynamics of complete, peeled, and cracked castor seeds were similar. In the first three days, the germination was slow, then it became faster. The germination rate of complete castor seeds and peeled castor seeds was not much, while the cracked castor seeds germination rate was about 10% lower than it. Endosperm damage of castor seeds germination was slow and germination rate was not high.

Table 1 showed the effect of the degree on mechanical damage on the germination rate and germination potential of castor seeds. The one-way ANOVA showed that mechanical damage had a significant effect on the germination rate and germination potential of the two varieties. By Duncan's multiple comparisons, the difference in germination rate between incompletely damaged castor seeds and cracked castor seeds was significant. The difference in germination rate between endosperm damaged castor seeds compared with complete castor seeds was highly significant. The difference of germination potential between damaged endosperm castor seeds and complete castor seeds was very significant. The germination rate of castor seeds with incomplete shell damage and cracked castor seeds were both 80%, but the germination potential of castor seeds with incomplete shell damage was 20% higher than that of cracked castor seeds.

It could be found that the germination rate of different damage types of castor seeds was significantly lower compared with complete after six days of germination test under the same environmental conditions. The seed shell damage could accelerate the germination of castor seeds, and endosperm damage seriously affected the germination and growth of castor seeds.

Table 1

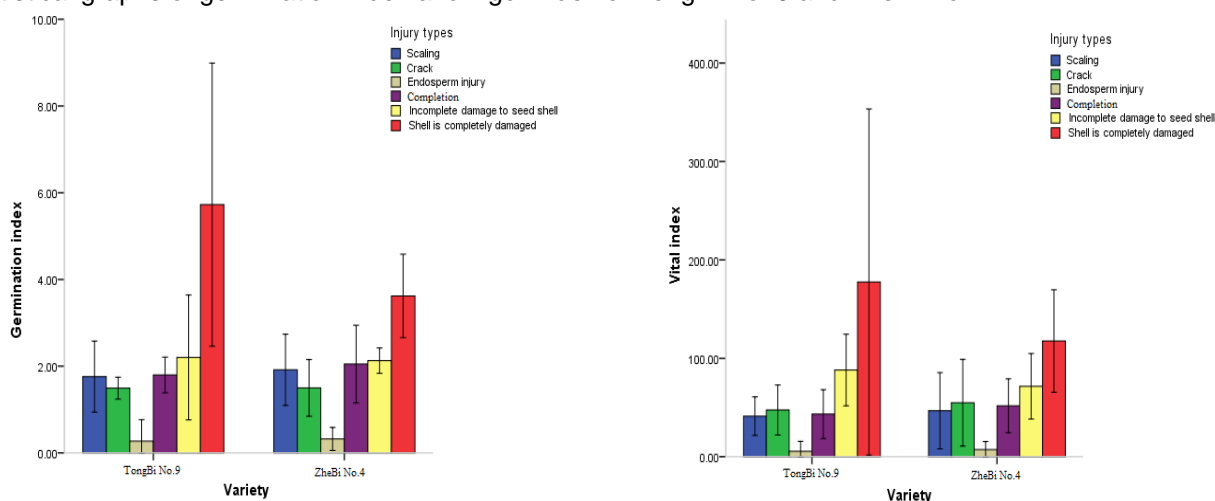
Effects of injury characteristics on germination rate and germination potential of castor oil seeds

Injury types	TongBi No.9		ZheBi No.4	
	Germination rate (%)	Germination potential (%)	Germination rate (%)	Germination potential (%)
Completion	96.67±5.77a	26.67±5.77bc	100.0a	23.33±5.77bc
Scaling	90.00±10.00ab	23.33±5.77bc	93.33±5.77ab	20.00±10.00bc
Crack	80.00±5.77b	13.33±5.77cd	76.67±11.55c	16.67±11.55cd
Incomplete damage to seed shell	80.00±10.00b	33.33±5.77b	86.67±5.77bc	33.33±5.77b
Shell is completely damaged	93.33±5.77ab	70.00±20.00a	96.67±5.77ab	53.33±5.77a
Endosperm injury	13.33±5.77c	3.33±5.77d	16.67±5.77d	6.667±5.77d

Note: Duncan's Multiple Range Test method was used for analysis, and different letters in the same column represented significant differences ( $P < 0.05$ ,  $n = 3$ )

Effect of damage on germination index vigor index

The germination index and vigor index of seeds were important indicators for seed vigor. Fig. 6 shows the statistical graphs of germination index and vigor index of TongBi No. 9 and ZheBi No.4.



a. Statistics of germination index for TongBi No.9 and ZheBi No.4

b. Statistics of vitality index for Tong Bi No.9 and ZheBi No.4

Fig. 6 - Statistics of germination index and vitality index for TongBi No.9 and ZheBi No.4

It could be found that the distribution of seed germination index and vigor index of the two varieties is the same. They are the highest for castor seeds with complete shell damage and the lowest for castor seeds with endosperm damage, which indicated that the difference between varieties on germination index and vigor index was not significant.

As shown in Table 2, the type of damage had a significant effect on the germination index and vigor index of both varieties. By Duncan's multiple comparisons, the difference in germination index between castor seeds with complete shell damage and castor seeds with endosperm damage was significant. The vigor index between cracked castor seeds, completely damaged castor seeds and complete castor seeds was highly significant. The germination index and vigor index of castor seeds with completely damaged seed shell were the highest, with a germination index of 5.73, 2.2 times higher than that of complete castor seeds. The vigor index of completed damaged shell is 177.55. While the germination index and vigor index of damaged endosperm seeds were the lowest, with a germination index of 0.32 and a vigor index of 7.28.

According to the results, the germination index vigor index is the highest when the seed shell is completely damaged. This indicated that its activity is the highest. The effect of endosperm injury on the germination index and vigor index of castor seeds is significant. So, the activity of castor seeds is seriously affected.

Table 2

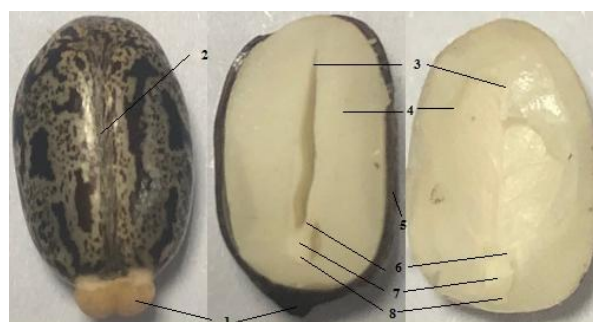
Effects of damage characteristics on germination index and vitality index of castor oil seeds

Injury types	TongBi No.9		ZheBi No.4	
	Germination index	Vital index	Germination index	Vital index
Completion	1.80±0.17b	43.26±9.99bc	2.05±0.36b	51.74±11.03b
Scaling	1.76±0.33b	41.21±7.91bc	1.92±0.33bc	46.72±15.58b
Crack	1.49±0.10b	47.47±10.23bc	1.50±0.26c	54.85±17.75b
Incomplete damage to seed shell	2.20±0.58b	88.08±14.66b	2.13±0.12b	71.57±13.38b
Shell is completely damaged	5.73±0.31a	177.55±70.79a	3.62±0.39a	117.54±20.96a
Endosperm injury	0.27±0.20c	5.51±4.07c	0.32±0.11d	7.28±3.29c

Note: Duncan's Multiple Range Test method was used for analysis, and different letters in the same column represented significant differences ( $P < 0.05$ ,  $n=3$ )

### The reasons for the low germination rate

The castor seed structure is shown in Fig. 7. The cracks and incomplete damage to the seed shell are seed shell breakage, and the germination site of castor seeds in the endosperm. It is known that the germination rate of cracked seeds and seed shells incompletely damaged seeds is 10% lower than the germination rate of castor seeds with completely fallen skin. Therefore, the cracked castor in seed and seed shell incomplete damage castor seeds needed to be dehulled to observe the internal conditions.



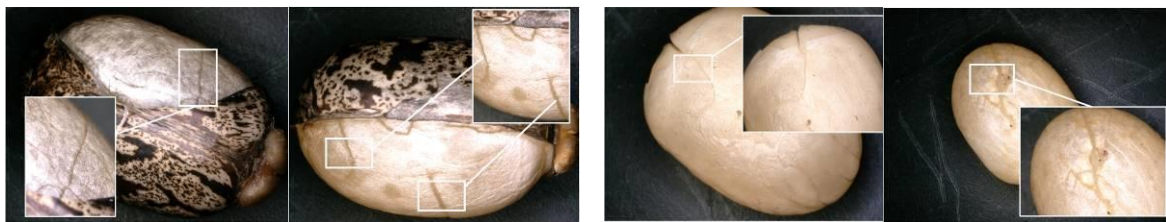
Shape Short diameter longitudinal section Long diameter longitudinal section

Fig. 7 - Structure of castor seeds

1.Caruncle; 2. Ridge; 3. Cotyledons; 4. Endosperm; 5. Seed shell; 6. Germ; 7. Hypocotyl; 8. Radicle

Fig. 8 shows the interior of the seed shells of both damage types, the small image in the image was a magnified view of the damage inside the defective image. It could be found that there are obvious cracks on the internal endosperm of castor seeds, indicating that the incomplete damage to the seed shell of castor seeds that did not germinate and cracked castor seeds also produced a certain amount of internal damage. The germination test found that when mechanical damage does not hurt castor seed endosperm, so mechanical damage could promote castor seed germination to some extent. When the mechanical damage is produced in castor seed endosperm and internal, mechanical damage would inhibit castor seed germination.

In this study, the number of castor seeds with completely damaged seed shells was less. According to the statistical results, the proportion of damaged castor seeds was less than 10%. The cracked castor seeds and seed shell incomplete damage castor seeds also contained 20-30% of endosperm damage castor seeds. Therefore, cracked castor seeds and castor seeds with incomplete damage to the seed shell were classified as damaged objects in the subsequent classification.



a. Incomplete damage to the interior of the seed shell

b. Cracked castor seed shell inside

Fig. 8 - Interior of the seed shell of two types of damage

### CRACK DETECTION ALGORITHM ON CASTOR SEEDS

#### Castor seed crack image

The castor seeds of ZheBi No.4 were selected as the test sample. The mechanical damage of castor seeds after shelling was surface cracking. Its common forms of cracking were lateral cracking text, abdominal cracking, and dorsal cracking, as shown in Fig. 9.



a. Lateral crack



b. Abdominal crack



c. Back crack

Fig. 9 - Cracks in different parts of castor seeds

#### Improved Canny algorithm

In this study, the maximum interclass variance method was applied, then the automatic threshold selection method of gradient magnitude histogram to find the low threshold of the image automatically. The gray levels after non-maximum suppression were divided into  $[0, L-1]$ , and the pixels in the edge map after non-maximum suppression were classified into three classes:  $C_0$ ,  $C_1$ ,  $C_2$ . The class  $C_0$  was for pixels that were not edge points. The class  $C_2$  was for pixels that were edge points, and class  $C_1$  contains pixels that might or might not be edge points. Set  $N$  to be the total number of pixels of modulus  $i$ , the number of pixels corresponding to gray level  $L-1$  to be  $n_i$ , and  $P_i$  to be the probability that the number of pixels of that gray level represents the number of pixels of the whole image.

$$P_i = \frac{n_i}{N} (i=1,2,3,\dots,L-1) \tag{5}$$

Let  $C_0$  contain pixels with amplitude gradients of  $[0, 1, \dots, k]$ .  $C_1$  contains pixels with gray levels  $[k+1, k+2, \dots, m]$ .  $C_2$  contains pixels with gray levels  $[m+1, m+2, \dots, L-1]$  of pixels, where  $k$  and  $m$  were low and high threshold values, respectively. The expectation of  $C_0$ ,  $C_1$ , and  $C_2$  were:

$$E_{C_0} = \frac{\sum_i^k i \cdot P_i}{\sum_i^k P_i} \tag{6}$$

$$E_{C_1} = \frac{\sum_k^m i \cdot P_i}{\sum_k^m P_i} \tag{7}$$

$$E_{C_2} = \frac{\sum_{l-1}^m i \cdot P_i}{\sum_{l-1}^m P_i} \tag{8}$$

The expectation for the entire interval was:

$$E = \frac{\sum_{l-1}^m i \cdot P_i}{\sum_{l-1}^m P_i} \tag{9}$$

The inter-class variance function could be defined as

$$\sigma^2 = (E_{C_0} - E)^2 + (E_{C_1} - E)^2 + (E_{C_2} - E)^2 \tag{10}$$

For a known graph,  $k$  and  $m$  could be found by the gradient histogram, and the variance in the maximum interclass variance method is denoted by  $\sigma^2$ . The superiority of interclass separability in the mathematical-statistical sense could be judged by maximizing the interclass variance. Therefore, the maximum value of  $\sigma^2$  could be found, and the values of  $k$  and  $m$  corresponding to its maximum value are the dividing points of the intervals  $C_0$ ,  $C_1$ , and  $C_2$ , which are also the high and low thresholds of the desired Canny operator. The result is shown in Fig.10.



Fig. 10 - Results of the improved algorithm

**Calculation of the length of crack defects in castor seeds**

**Calibration of objects**

In this study, a square standard block was used with the upper surface of 1 cm side length to calibrate the object based on the correspondence between the pixel value of the standard block and the actual size. The original image of the calibration block is shown in Fig. 11.



Fig. 11 - Original image of calibration block



Fig. 12 - Actual measured crack length

According to the Canny edge detection, the perimeter pixel of the calibration block was 3526. The crack length pixel obtained by the edge detection algorithm with the Canny operator was 698. The multiple calibrators could make the actual size represented by the pixel more accurate. The values of its multiple calibration blocks are shown in Table 3. As shown in Fig. 12, the actual length of castor seed cracks measured according to the length measurement function of the super depth-of-field microscope was plotted, then the actual length of cracks  $L_1$  was measured. The pixel to actual size relationship of the calibration block is calculated by equation (11).

$$A = \frac{l}{P} \tag{11}$$

Where:  $A$  is the actual size represented by a pixel value ( $\mu\text{m}\cdot\text{px}^{-1}$ ).  $l$  is the actual size of the calibration block ( $\mu\text{m}$ ).  $P$  is the pixel value of the calibration block ( $\text{px}$ ).

Table 3

Multiple calibration block pixels represent actual size values

	Object description 1	Object description 2	Object description 3
A/um-px <sup>-1</sup>	11.76	11.68	11.71

When several calibration blocks of pixels representing the actual size were found, the average value was taken to make the calculation easier. The actual length of the crack  $L_2$  was obtained by calculation as 8181 um. The actual crack length detected was compared with the length measured by the ultra-field microscope, the error of which was 23.46%. Fig.13 shows a graph of the crack treatment for recording some of the castor seeds. Table 4 shows the comparison between the actual length of crack detection and the length measured by the deep field microscope for castor seeds.



Fig. 13 - Castor seed crack treatment results comparison diagram

Table 4

Surface crack length of castor seeds

Number	Actual crack length/um	Measures length/um	Error/%
1	8181	10688	23.46
2	7258	7971	8.94
3	2076	2686	23.71
4	5177	6871	24.65
5	5083	6144	17.27
6	2073	2654	21.89
7	809	1001	19.18
8	3871	5316	27.18

There were many factors in the process of crack identification that could affect the results. The castor seeds have grayish-white and dark brown or yellowish-brown patterns on the surface, and the cracks were similar in color to the patterns. The computer can incorrectly identify the patterns as cracks in the identification process, which would lead to large errors in the results. The surface of castor seed is curved in the light to produce shadows, projected on the outer contour of the castor seed. The edge of the outer contour is partially covered by shadows, resulting in the detection of its area being smaller than its actual area.

ALGORITHM STUDY OF CASTOR SEEDS WITH SEED SHELLS

Image of castor seeds with missing seed shells

Seed shell loss was a serious problem during the shelling process of castor capsules. It resulted in the breakage and loss of the outer seed shell of castor seeds, exposing the inner white endosperm directly to the air. Fig. 14 shows the image of castor seed after seed shell loss.



Fig. 14 - Lack of castor seeds in shells

**Threshold segmentation**

In this study, the automatic threshold selection method with the maximum variance between classes was used in image thresholding, which was based on the grayscale distribution of the image. It calculated the grayscale histogram classes of the background and the target under different thresholds by traversing. Then by comparing the variance between the background and the target, the variance was maximized.

**Area calibration and calculation**

Each parameter of the super deep field microscope was adjusted: the castor seeds were placed directly below the microscope camera, a suitable shooting distance was selected, and the focal length and aperture of the microscope were adjusted to make the sharpest images of the collected castor seed samples. Secondly, a rectangular standard block with an upper surface of 1.1 cm x 0.9 cm was applied in this study to calibrate the object based on the correspondence between the pixel value of the standard block and the actual size. The original image of the area calibration block is shown in Fig.15.



Fig. 15 - Image of area calibration block



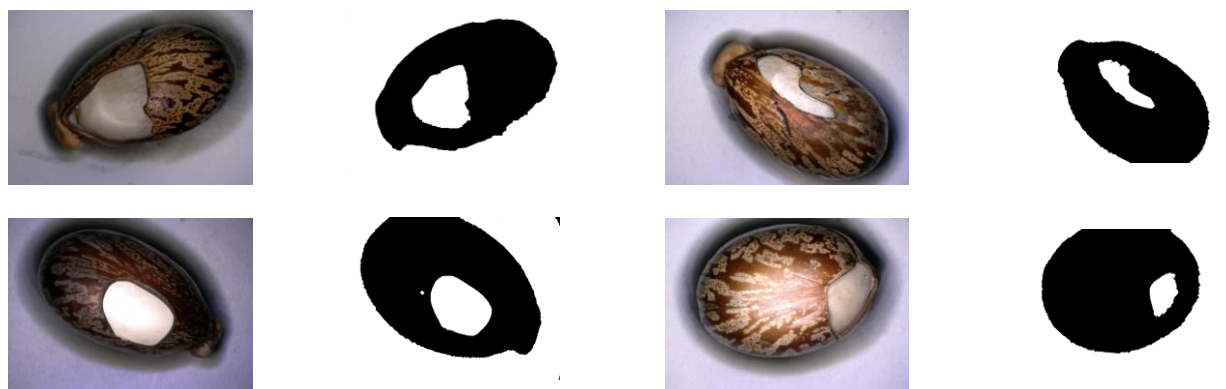
Fig. 16 - Absence of actual measured area of the seed shell

After morphological processing, the area pixels of the calibration block were 731108 and the area pixels of the seed shell missing castor seed map obtained with the maximum interclass variance algorithm was 157302. As shown in Fig. 16, the area map was measured with the super deep field microscope device. The actual area of the missing seed shell  $S_1$  was measured, which is 24977950  $\mu\text{m}^2$ . The relationship between the pixels of the calibration block and the actual size is calculated according to equation (12).

$$a = \frac{S}{P} \tag{12}$$

Where:  $a$  is the actual area size represented by a pixel value ( $\mu\text{m}^2 \cdot \text{px}^{-1}$ ).  $S$  is the actual size of the calibration block ( $\mu\text{m}$ ).  $P$  is the pixel value of the calibration block ( $\text{px}$ ). According to the formula,  $a$  is 135.411.

The defect area extraction was performed by the maximum interclass variance algorithm for seed shell defective castor seed images with different parts of defects. The different images are enumerated as shown in Fig. 17 below.



(a) Absence of castor seed image in the seed shell

(b) Processed image

(a) Absence of castor seed image in the seed shell

(b) Processed image

Fig. 17 - Results of castor treatment without castor seeds of different species

**Comparison of the missing area of castor seed shell surface** **Table 5**

Number	Area of pixels	Actual area / $\mu\text{m}^2$	Measures area / $\mu\text{m}^2$	Error / %
1	157302	21300421	24977950	14.72
2	78983	10695167	10877339	1.68
3	145846	19749153	18130755	-9.38
	608	82330		
4	66235	8968948	11238750	20.20
5	86772	11749883	14332479	18.02
6	61098	8273341	8668171	4.55

From Table 5, it could be calculated that the minimum error of castor seeds with seed shell missing was 1.68% and the larger error was 20.20%. However, seed shell missing defects in the recognition process would have many factors that affect the extraction of defective features, part of which had the phenomenon of skin loss connected with defects, resulting in a smaller detection area than the actual area. The castor seed defects were too close to the edge, which resulted in a smaller detection area than the actual area. The castor seeds had a smooth surface, which would reflect the light.

## CONCLUSIONS

The single factor experimental analysis shows that the mechanical damage has a significant effect on the germination rate, germination potential, germination index, and vigor index of castor seeds. The germination rate and germination potential of castor seeds with complete shell damage are the highest, with 93% germination rate and 70% germination potential. The germination rate of castor seeds with incomplete shell damage and cracked castor seeds are both 80%, but the germination potential of castor seeds with incomplete shell damage is 20% higher than that of cracked castor seeds.

It is found that there are two types of damage castor seed internal endosperm, which are single crack and turtle crack. Then the other forms of cracks produced is the same. The endosperm damage germination rate is 20%, which seriously affected the germination rate of castor seed and its germination quality. The cracked castor seed and seed shell incompletely damaged castor seed germination rate was 10% lower than the germination rate of intact castor seeds.

Comparing the detection of the actual crack length with the length measured by the super deep field microscope, it could be found that the error range was basically around 25%, and the better error was around 10%. The image segmentation of castor seeds with missing seed shells by the maximum variance method and the morphological processing could completely extract the features of seed shell missing castor seed images. The error between the extracted feature area and the actual measured object area function of the super-field microscope is around 10%.

## ACKNOWLEDGEMENT

This research is supported by the National Natural Science Foundation of China, China (51457312), the authors thank relevant scholars for their assistance in the literature.

## REFERENCES

- [1] Che W.K., Sun L.J., Zhang Q., Tan W.Y., Ye D.D., Zhang D., Liu Y.Y., (2018), Pixel based bruise region extraction of apple using Vis-NIR hyperspectral imaging. *Computers & Electronics in Agriculture*, Vol.146, pp.12-21;
- [2] Cheng L., (2018), *Apple surface defect detection research based on improved particle swarm optimization algorithm*. *Food & Machinery*, Vol.34, Issue 03, pp.141-145.;
- [3] Chiara L.P., Dana Z., Agata L., Daniela B., Fabio P., Pietro F., Brijesh T., Paula B., Cullen P.J., (2018), Plasma activated water and airborne ultrasound treatments for enhanced germination and growth of soybean. *Innovative Food Science & Emerging Technologies*, Issue 49, pp.13-19;
- [4] Diao Z.H., Diao C.Y., Yuan W.B., Wu Y.Y., (2018), Threshold segmentation algorithm for wheat diseased spot based on improved fuzzy edge detection. *Transactions of the Chinese Society of Agricultural Engineering*, Vol.34, Issue 10, pp. 147-152;

- [5] Gao L.X., Li X.F., Jie X., Na X.J., Zhang W., Du X., (2010), Effects of internal mechanical damage on germination of soybean. *Transactions of the Chinese Society for Agricultural Machinery*, Vol.41, Issue 10, pp.63-66+102;
- [6] Gu R.L., Huang R., Jia G.Y., Yuan Z.P., Ren L.S., Li L., Wang J.H., (2019), Effect of mechanical threshing on damage and vigor of maize seed threshed at different moisture contents. *Journal of Integrative Agriculture*, Vol.18, Issue 07, pp.1571-1578;
- [7] Han Y., Chu Z., Zhao K., (2020), *Target positioning method in binocular vision manipulator control based on improved canny operator*. *Multimedia Tools and Applications*, Vol.79, pp.9599-9614.;
- [8] Henila M., Chithra P., (2020), Segmentation using fuzzy cluster-based thresholding method for apple fruit sorting. *IET Image Processing*, Vol.14, Issue 16, pp.4178-4187;
- [9] Joanna P., Agnieszka S., Agnieszka S., Piotr Y., Michal K., Malgorzata B., Dariusz A., (2018), Effects of atmospheric pressure plasma jet operating with DBD on *Lavatera Thuringia L.* seeds' germination. *PLOS ONE*, Vol.13, Issue 04, pp.1-12;
- [10] Ju S., Bo K., Chla B., (2020), Breaking combinational dormancy of *Rhus javanica L.* seeds in South Korea: Effect of mechanical scarification and cold-moist stratification. *South African Journal of Botany*, Vol.133, pp.174-177;
- [11] Ju S.C., Lee C.H., (2018). Effect of germination and water absorption on scarification and stratification of kousa dogwood seed. *Horticulture Environment & Biotechnology*, Vol.59, Issue 03, pp.1-10;
- [12] Ju Z.Y., Xue Y.J., Zhang W.X., Zhai C.Y., (2020), Pomegranate Disease Spot Detection Algorithm Based on Adaptive Threshold Prewitt. *Transactions of the Chinese Society of Agricultural Engineering*, Vol.36, Issue 08, pp.135-142;
- [13] Junior F.G., Cicero S.M., Vaz C., Lasso P., (2019), X-ray microtomography in comparison to radiographic analysis of mechanically damaged maize seeds and its effect on seed germination. *Acta Scientiarum Agronomy*, Vol.41, pp. e42608;
- [14] Li J.W., Zhou R.W. Zhou R.S., Zhang X.H., Yang S.Z., (2018), Atmospheric-pressure plasma-treated water for seed germination and seedling growth of mung bean and its sterilization effect on mung bean sprouts. *Innovative Food Science & Emerging Technologies*, Issue 53, pp.36-44;
- [15] Li J.Z., Zhang B.X., Wang W.N., Hou X.Y., Liu H.G., Yang Y.F., Tang D.Y., Wang G.M., (2018), Research progress in breeding and cultivation of castor in China. *Bulletin of Agricultural Science and Technology*, Issue 10, pp.198-200,2;
- [16] Li Y.N., Sun J., Ding Q.S., Liu Y.Y., Ding W.M., (2015), Effects of glumes and cracks on seed germination and seedling growth of hybrid rice. *Hybrid Rice*, Vol.30, Issue 04, pp.71-74;
- [17] Liu L.B., Cheng X.L., Dai J.G., Lai J.C., (2017), Adaptive Threshold Segmentation of Cotton Field Canopies Image Based on Logical Regression Algorithm [J]. *Transactions of the Chinese Society of Agricultural Engineering*, Vol.33, Issue 12, pp.201-208;
- [18] Liu Y.X., Su B.F., Wang C., Mi Z.W., Wang F.Y., (2019), Leaf area estimation method based on three-dimensional point cloud. *Transactions of the Chinese Society for Agricultural Machinery*, Vol.50, Issue 12, pp.240-246+254;
- [19] Luo W., Zhang H., Liu X., (2019), Hyperspectral/Multispectral Reflectance Imaging Combining with Watershed Segmentation Algorithm for Detection of Early Bruises on Apples with Different Peel Colors. *Food Analytical Methods*, Vol.12, Issue 05, pp.1218-1228;
- [20] Sangeetha D., Deepa P., (2016), FPGA implementation of cost-effective robust Canny edge detection algorithm. *Journal of Real-Time Image Processing*, Vol.16, pp.957-970;
- [21] Song Y.Q., Jiao J.K., Wu L.Y., Chi B.W., Chen T.Y., Zhang B.F., Lu C.Z., Xin M.J., (2019), Effects of mechanical compression on emergence and growth of garlic seed flap. *Transactions of the Chinese Society of Agricultural Engineering*, Vol.35, Issue 05, pp.26-32;
- [22] Wang G., Tse P.W., Yuan M., (2017), Automatic internal crack detection from a sequence of infrared images with a triple-threshold Canny edge detector. *Measurement Science and Technology*, Vol.29, pp.025403;
- [23] Yang Y., Zhao X., Huang M., Zhu Q; (2021), Multispectral image-based germination detection of potato by using supervised multiple threshold segmentation models and Canny edge detector. *Computers and Electronics in Agriculture*, Vol.182, Issue 07, pp.106041;
- [24] Yu S.C., Li Y.M., Ma Z., Wang J.T., Hu B.Y., Xu L.Z., Tang Z., (2019), Study on the morphology of grain and cob damage during direct harvesting of maize. *Journal of Agricultural Mechanization Research*, Vol.41, Issue 10, pp.208-212.